Laser-induced fluorescence measurements of ion fluctuations in electron and ion presheaths

Cite as: Phys. Plasmas **27**, 053509 (2020); https://doi.org/10.1063/1.5142014
Submitted: 09 December 2019 . Accepted: 24 April 2020 . Published Online: 12 May 2020

R. Hood, S. D. Baalrud, R. L. Merlino, F. Skiff, et al.

Physics of Plasmas ARTICLE scitation.org/journal/php

Laser-induced fluorescence measurements of ion fluctuations in electron and ion presheaths

Cite as: Phys. Plasmas **27**, 053509 (2020); doi: 10.1063/1.5142014
Submitted: 9 December 2019 · Accepted: 24 April 2020 ·
Published Online: 12 May 2020

R. Hood,[a] S. D. Baalrud, R. L. Merlino, and F. Skiff

AFFILIATIONS

Department of Physics and Astronomy, University of Iowa, Iowa City, Iowa 52242, USA

[a]Author to whom correspondence should be addressed: rthood@sandia.gov

ABSTRACT

Electrostatic flow-driven instabilities have been predicted in the presheath region of low-temperature plasmas for both ion and electron rich sheaths. The ion-acoustic fluctuations that arise from these instabilities can influence transport through an enhanced collision rate. In this work, ion fluctuation spectra were measured using laser-induced fluorescence (LIF) in the presheath region for both sheath polarities. The non-invasive nature of LIF compared to that of probes is particularly valuable for these measurements because the sheath and presheath around a probe may generate their own flow-driven instabilities, which obscure the measurement. Measurements were made using a recently implemented field programmable gate array-based system able to measure ion fluctuation spectra up to 1 MHz using a two-point correlation function technique. Narrow bandwidth ion fluctuations were observed near $0.46 f_{pi}$ (460 kHz) for both sheath polarities, where f_{pi} is the ion plasma frequency. The observed fluctuations were significantly stronger in the electron sheath case and were observed over a larger volume of plasma. Fluctuations were measured in the ion sheath case at locations far enough from the sheath that linear theory predicts stability, suggesting that ion-acoustic instabilities generated in the relatively small unstable region near the boundary reflect from the sheath and perturb a much larger volume of the plasma. This is expected to affect probes with both ion and electron rich sheaths, meaning any dc biased probe may effectively act as an ion-acoustic wave antenna. These measurements are consistent with the recent theory and particle-in-cell results.

I. INTRODUCTION

Sheaths play an important role in bounded plasmas by governing the loss of charged particles from the system. Instabilities in the boundary region are generally not considered; however, the presheath is susceptible to ion–electron streaming instabilities that can influence transport through instability-enhanced collisions.[1–3] A modification to the collision rate in the presheath is expected to impact many important applications, such as modeling of steady-state plasma conditions and plasma–surface interactions, as well as the interpretation of Langmuir probe and other probe-based measurements.

Measurements of the fluctuations generated by these instabilities have, until now, been limited to probe-based diagnostics[4] and particle-in-cell (PIC) simulations.[2,5] Probe-based measurements of this kind are not ideal because the sheath and presheath around a probe may generate their own flow-driven instabilities, which obscure the measurement. In this paper, non-perturbative measurements of these fluctuations, collected using laser-induced fluorescence (LIF), are presented for the first time. Narrow bandwidth ion fluctuations were observed near $0.46 f_{pi}$ (460 kHz) for both ion and electron sheaths, where $f_{pi} = (4\pi ne^2/m_i)^{1/2}/2\pi$ is the ion plasma frequency.

In low-temperature plasmas, electrons generally have a greater mobility than ions. As a result, most sheaths in these systems are ion rich so that the sheath potential gradient repels most electrons, allowing the bulk plasma to remain quasineutral. The sheath potential gradient also produces an ion flow toward the boundary. At steady-state, this flow must satisfy the Bohm criterion,[6] which requires that ions enter the sheath at the ion sound speed $c_s = \sqrt{T_e/m_i}$. To satisfy this requirement, a quasineutral presheath region accelerates ions through a small potential drop of approximately $T_e/2e$ over a much larger-scale region than the sheath, which is often associated with the ion-neutral mean free path.[7,8] Electrons in the presheath do not develop a flow-shift and follow a Boltzmann density distribution.[6] Examples of typical ion sheath and presheath potential profiles can be observed in Fig. 3 for cases where the boundary potential ϕ_{El} is negative relative to the plasma potential ϕ_p.

The presheath is susceptible to streaming instabilities due to the flow-shift between ion and electron velocity distributions in this region. Instability-driven ion-acoustic fluctuations are predicted to occur when the flow-shift V_i exceeds a threshold value dependent on the electron to ion temperature ratio and neutral gas pressure.[1] The

ion-acoustic waves generated are predicted to propagate toward the boundary at approximately the ion sound speed. The frequency of observed plasma fluctuations and instability threshold may be predicted by evaluating the standard approximate dispersion relation for flow-shifted Maxwellian ions and electrons in the ion plasma frequency range; see, for example, Eqs. (7) and (8) of Ref. 1. For our experimental conditions where an ion rich sheath is present, this yields a threshold flow-shift of approximately $0.5c_s$, which is exceeded for the last ~1 cm of the presheath up to the sheath edge.

Plasma fluctuations have been predicted to result in instability-enhanced collisions.[9,10] This may account for anomalous ion thermalization sometimes observed in the sheath and presheath.[11] Evidence of this effect has been observed in the ion presheath through measurements of the thermalization of the ion velocity distribution function (IVDF) using LIF.[3] These measurements agree well with the predicted stability threshold for ion-acoustic instability as a function of neutral pressure. However, they only provide indirect evidence for the existence of the instability. In this work, we provide direct evidence for this instability through LIF measurements of ion fluctuation spectra.

While sheaths are typically ion rich, electron rich sheaths are also possible, provided the boundary surface is biased positive with respect to the plasma potential. Electron sheaths have an inverted potential structure compared to ion sheaths, as can be seen in Fig. 3. This is only possible near boundaries with a sufficiently small electron collection area compared to the area of other boundaries that collect ions.[12] Electron sheaths are most commonly encountered on Langmuir probes biased for electron saturation, but are also found in many other applications such as scrape-off layer control surfaces in fusion devices,[13,14] electron temperature control surfaces in laboratory plasmas,[15] and retarding field ion energy analyzers, which are utilized in a wide range of applications, including fusion devices[16,17] and plasma processing.[18]

Due to the comparative rarity of electron sheaths, they have not been studied as thoroughly as their ion rich counterparts. Recent publications have suggested that the conventional theory for the electron sheath is incomplete. The conventional theory implies that no presheath is necessary, since the electron sheath is assumed to collect a random flux of boundary-directed electrons.[19,20] This results in a truncated electron velocity distribution at the sheath edge that trivially satisfies the electron sheath analog of the Bohm criterion.[21,22] Recent theoretical work[2] along with particle-in-cell simulations[2,5,23] has suggested that there is a presheath region through which the electrons develop a flow-shift V_e, ultimately reaching the electron thermal speed $v_{te} = \sqrt{T_e/m_e}$ at the sheath edge. The electron presheath is predicted to be much longer than an ion presheath. In practice, the predicted length often exceeds the dimensions of experimental devices, in which case the presheath is expected to fill approximately half the experiment length.[2]

Streaming instabilities are predicted in the modified electron sheath theory, similar to those predicted in the ion presheath.[1,2] However, in this case, it is the electrons that are flowing and the ions do not develop any significant flow.[2,23,24] Fluctuations are expected to become stronger and occur much farther from the boundary in the electron presheath since it is predicted to generate much stronger flow-shifts over longer spatial scales. The frequency of the observed plasma fluctuations and instability threshold may be predicted by evaluating the approximate dispersion relation for flow-shifted Maxwellian ions and electrons where the flow-shift is assumed to be large compared to the ion sound speed $V_e \gg c_s$; see Eq. (23) of Ref. 2. In this case, the flow is predicted to be unstable throughout the majority of the presheath, which is expected to fill much of the plasma volume in our experiment of ~20 cm. The ion-acoustic waves generated are predicted to propagate toward the boundary at approximately the ion sound speed. The additional distance over which waves propagate along with the larger growth rate provides the opportunity for waves to grow to larger amplitude in the electron presheath, although it is likely that the wave amplitude saturates before reaching the boundary.[2] As in the ion sheath case, the fluctuations are expected to result in instability-enhanced collisions, which would likely be the dominant collision mechanism for electrons in the presheath and could be the process ultimately responsible for determining the presheath length scale. Observation of ion-acoustic fluctuations in the electron presheath would provide evidence in favor of the modified electron sheath theory since the random flux model of the conventional theory is predicted to be stable. Indeed, fluctuations are often associated with positively biased probes and have been observed in PIC simulations[2,5] and probe measurements.[4] These experimental measurements showed fluctuations in the current collected by a positively biased electrode. While non-invasive, this technique gives no spatial resolution within the plasma and only involves electrons, which may not be representative of ion behavior. The spatially resolved LIF fluctuation measurements of this work improve on these measurements and are a test for the modified theory for the electron sheath.

Ion fluctuations were observed for both ion and electron sheaths under low-temperature plasma conditions using a newly developed LIF diagnostic system. The fluctuation strength was observed to increase for electrode biases above the plasma potential, corresponding to the transition from ion to electron sheath. In addition, spatially resolved measurements of the electron presheath region show that the fluctuation amplitude decreases slowly over the measurement range. These measurements are consistent with the modified theory for the electron sheath, which predicts the presence of a long-range electron presheath on the scale of the experiment dimensions.[2] The fluctuations observed are consistent with ion-acoustic fluctuations and were at a frequency near $0.46f_{pi}$ for each configuration, consistent with predictions from the dispersion relations. In the ion sheath case, fluctuations were observed outside of the predicted unstable region, suggesting that wave reflection may play a significant role. Reflection suggests that instabilities excited near the electrode, which were previously assumed to be a local phenomenon, actually influence a much larger volume of the plasma surrounding the electrode. Finally, a comparison between fluctuation measurements made using LIF and the current collected by the electrode shows similar trends but quantitatively very different behavior (a factor of ~10 difference in the fluctuation power).

II. EXPERIMENT DESCRIPTION

Argon plasma was produced in a multidipole chamber through impact ionization by primary electrons emitted from a hot cathode biased near −110 V with respect to the grounded chamber walls (see Fig. 1). The cathode consisted of a sintered lanthanum-hexaboride (LaB_6) ring segment that was heated resistively and was located on one of the chamber end-caps, approximately 30 cm from the biased electrode at the center of the chamber. The multidipole confinement consisted of a magnet cage with 16 rows of magnets with alternating poles

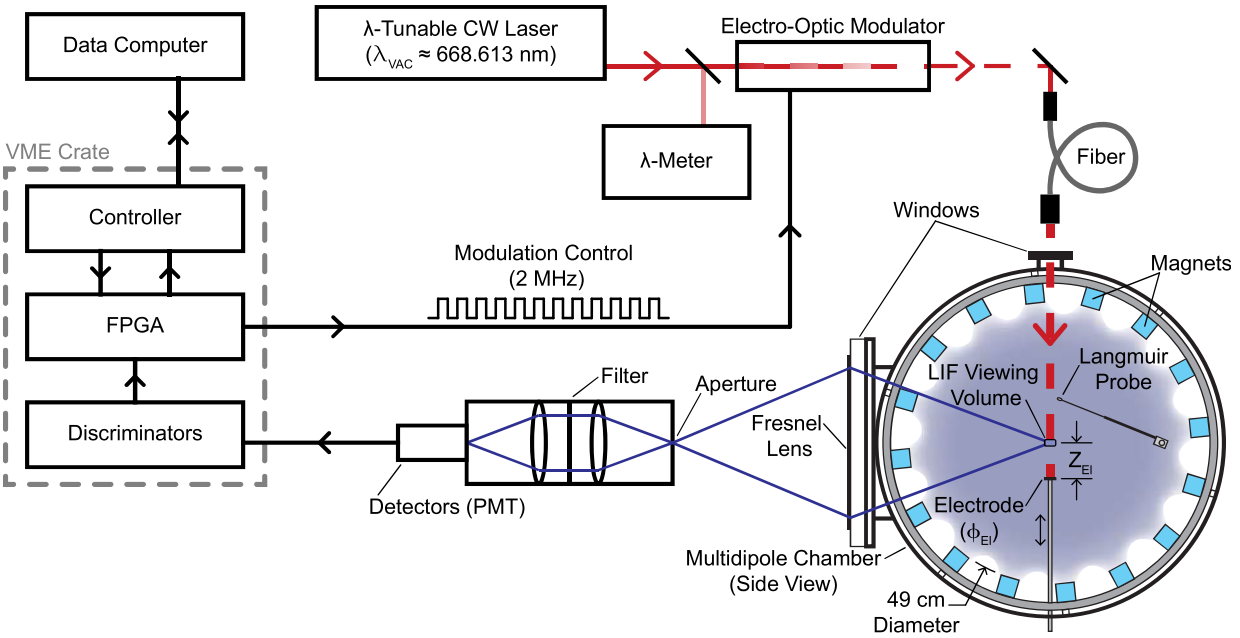

FIG. 1. Experimental schematic showing the LIF system and a side view of the multidipole chamber. The hot cathode plasma source (not shown) was located on one of the chamber end-caps, near the center of the chamber radially (∼30 cm from the electrode). Modulated laser light was injected through a window on top of the chamber onto the biased electrode. Fixed LIF optics collected light from a volume of plasma above the electrode surface near the center of the chamber. The electrode surface, biased to a potential ϕ_{EI} with respect to the plasma potential ϕ_p, was translated up and down to vary the separation Z_{EI} between the electrode and the viewing volume. An array of 32 photomultiplier tube (PMT) detectors observed the collected fluorescence. The collected signals were demodulated and summed up by the FPGA before being sent to the data computer for analysis.

covering all inside walls of the chamber and was electrically connected to the grounded chamber walls. The inner dimensions of the magnet cage were 73 cm long × 49 cm diameter. The maximum field strength was approximately 1000 G near the surface of the magnets and 2 G in the measurement region. Measurements were made near a 1.9 cm diameter stainless steel electrode on a translatable shaft inserted from the bottom of the chamber. The electrode surface was made from a thin razor blade stack that acted as a beam dump for the laser. The sides of the electrode were also conductive in order to minimize flows generated by ion sheaths associated with a dielectric material that may perturb measurements.[24] The neutral pressure in the chamber was regulated using a mass flow controller set to 0.30 sccm of argon, resulting in a constant pressure of 1.4×10^{-5} Torr. The system base pressure was less than 10^{-6} Torr.

The shape of the fluctuation peak on the power spectrum was found to be sensitive to the specific conditions of the discharge, such as neutral pressure and primary electron energy and current. Numerous peak shapes were observed using the spectrum analyzer, including narrow, broad, double, as well as peaks that were not stationary. However, to produce the best LIF measurements so that the total fluctuation power could be compared between electrode configurations, the heating current and emission bias on the plasma source were adjusted slightly (<5%) between each configuration to produce a strong instability with a narrow bandwidth at 460 kHz. This specific peak frequency and neutral pressure were chosen because they were found to give a consistent and strong peak shape over a wide range of electrode biases and positions. The frequency of the instability peak was observed to be proportional to the ion plasma frequency (Fig. 2), as predicted by the theory.

The principal controls for adjusting the discharge parameters were the current and energy of the primary electrons from the hot cathode source. The product of the primary electron current and the primary electron potential relative to the plasma potential is the total discharge power. The discharge power was nearly constant between configurations; however, small changes were made for two purposes. First, the effective loss area for the plasma was modified slightly as the electrode bias and position were changed. Thus, the discharge power was slightly changed to maintain a constant plasma density. Second, since the instability bandwidth was approximately 2 kHz when the peak frequency was 460 kHz, the density needed to remain constant in time throughout the LIF acquisition to within 1% to keep the instability frequency from shifting by more than the fluctuation bandwidth. Since the experiment does not have this level of stability over the course of hours, active feedback was applied to the plasma source heating and bias to hold the instability peak at a constant 460 ± 2 kHz. Still, this did result in broadening of the LIF spectra, but is expected to be consistent between runs and to not affect the integrated fluctuation power.

The ion density and electron temperature were measured using a 6 mm diameter Tantalum disk-shaped Langmuir probe located 8 cm from the LIF viewing volume and approximately 10–20 cm from the biased electrode (see Fig. 1). The plasma potential was measured with an emissive probe using the floating point in the limit of a high emission technique.[25] The sheath structure was measured for each

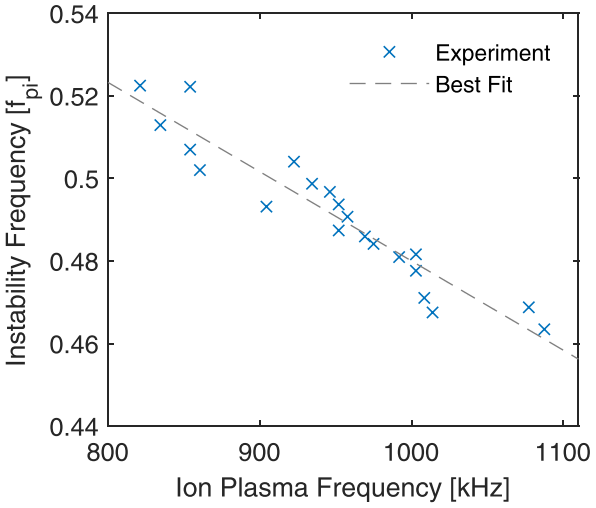

FIG. 2. Peak instability frequency plotted as a function of the ion plasma frequency. Measurements were made using a spectrum analyzer that observed the current collected by a positively biased electrode as the plasma density was adjusted from 6.1×10^8 cm^{-3} to 1.1×10^9 cm^{-3}. The density was measured using a Langmuir probe approximately 15 cm from the electrode surface. The data follow a linear trend with a slope of -2.16×10^{-7} and a y-intercept of 0.70. The plotted data do not contain points from the fluctuation measurements that are the focus of this work, since those were collected under different experimental conditions. Nevertheless, those measurements are in good agreement, with instability frequencies near 0.46 f_{pi} for ion plasma frequency near 1 MHz.

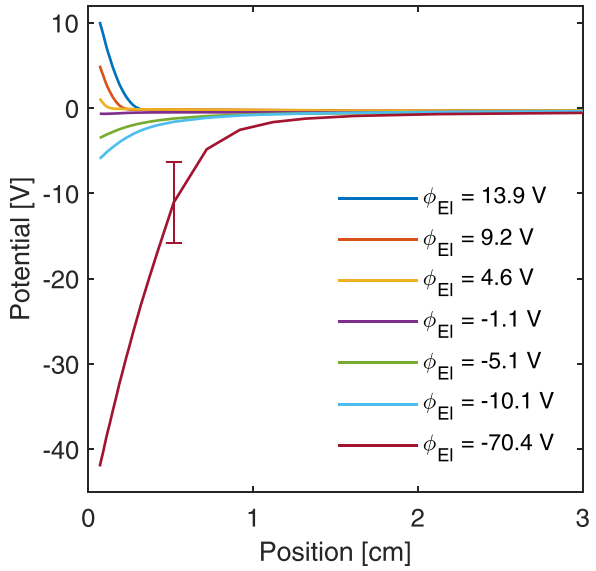

FIG. 3. Emissive probe measurements of plasma potential as a function of distance from the electrode surface for each electrode bias tested. Measurements extend to 15 cm, but are flat beyond ∼2 cm. All potentials in this figure are relative to the bulk plasma potential, which is $\phi_p \approx -7$ V relative to ground. An error bar is shown indicating the accuracy of the measurement $\sim T_e/e \approx 4.8$ V. The precision of the measurement is much better at ∼0.2 V.

electrode bias using the emissive probe at the center of the chamber. The plasma potential was measured as a function of distance from the electrode surface as the electrode was retracted from the chamber. The emissive probe was retracted during LIF measurements so as to not perturb the measurement region. Spatially resolved plasma potential measurements are shown in Fig. 3. Plasma density, potential, and electron temperature are given in Table I for each configuration tested.

LIF fluctuation measurements were collected with the electrode in 11 different configurations outlined in Table I. These consisted of seven electrode bias values with the center of the LIF observation volume held 6 cm from the electrode surface, as well as three additional electrode positions with the bias held 9 V above the plasma potential, and one final configuration with the electrode electrically floating and withdrawn as far from the LIF observation volume as possible (16.2 cm from the viewing volume). In addition to the LIF measurements, power spectra of the current collected by the electrode were recorded using a TELEDYNE LECROY HDO 4104 oscilloscope operating as a spectrum analyzer, which observed the voltage across a 50 Ω resistor in series with the electrode bias power supply.

TABLE I. Experimental configurations tested. The separation Z_{El} between the center of the LIF observation volume and the electrode surface, the potential ϕ_{El} of the electrode surface, plasma potential ϕ_p, ion density n, electron temperature T_e, and the velocity of ions resonant with the laser V_D (relative to the IVDF center) are given. In configuration 11, the electrode was electrically floating, corresponding to a potential of approximately −30 V relative to the plasma potential. The laser wavelength was chosen to excite ions with velocities in the direction of the boundary.

Configuration	Z_{El} (cm)	ϕ_{El} with respect to ϕ_p (V)	ϕ_p wrt ϕ_{Wall} (V)	n (cm^{-3})	T_e (eV)	V_D (v_{Ti})
1	6.0	13.9	−6.6	8.8×10^8	4.9	1.05
2	6.0	9.2	−6.8	8.9×10^8	4.9	1.08
3	3.0	9.2	−6.8	8.9×10^8	4.9	1.01
4	1.5	9.1	−6.8	9.1×10^8	4.9	1.01
5	12.0	8.9	−6.8	8.9×10^8	4.8	1.09
6	6.0	4.6	−7.3	9.2×10^8	4.7	0.85
7	6.0	−1.1	−7.6	9.4×10^8	4.8	0.87
8	6.0	−5.1	−7.9	9.3×10^8	4.8	0.99
9	6.0	−10.1	−8.0	9.5×10^8	4.7	1.04
10	6.0	−70.4	−8.1	8.7×10^8	4.9	0.94
11	16.2	Floating	Not measured	9.7×10^8	4.6	1.09

III. LIF DIAGNOSTIC

LIF is typically used to make non-perturbative measurements of the IVDF by observing the magnitude of the fluorescence signal as a laser is tuned across the Doppler-broadened metastable ion transition, allowing time-averaged fluid moments to be computed (density, flow, temperature, and so on).[26] However, LIF also enables non-perturbative measurements of ion fluctuation spectra by recording a time resolved fluorescence signal.[27–30] For these measurements, the laser wavelength is typically fixed so that ions with velocities near the ion thermal speed $v_{ti} = \sqrt{T_i/m_i}$ are selected. This is where the fluctuation signal is the largest (for ion-acoustic waves) and corresponds to the inflection point on the IVDF for Maxwellian velocity distributions. This technique provides clear benefits over probe-based measurements due to its non-perturbative nature. However, ion fluctuation spectra are challenging to obtain using LIF due to two major sources of photon statistics noise inherent to the diagnostic. The first is the fluctuating background light that makes up approximately 99% of the light collected. This is caused by plasma light, primarily collisionally-induced fluorescence, near the wavelength of the LIF transition passing through the optical filters in the collection system. The second source of noise is due to the limited LIF photon count rate resulting from the low metastable state density, finite observation volume, and the desire to avoid optical pumping at high laser power.[31]

These sources of noise are addressed using the traditional LIF technique of laser amplitude modulation along with a two-point correlation technique. Rapidly modulating the laser amplitude between "ON" and "OFF" reduces noise by enabling the background light level to be subtracted while providing time resolved measurements at a rate limited to the modulation frequency. We utilize a two-point correlation technique between two overlapping diagnostic volumes. The ensemble averaging utilized in this correlation technique suppresses the photon statistic noise floor since the photon statistic fluctuations are uncorrelated between the separate detection paths. This technique has been utilized in numerous experiments to measure ion fluctuation spectra using LIF with a spectral bandwidth of up to 50 kHz.[27–29] In this work, we measure fluctuations with frequencies near 500 kHz, requiring some changes to the LIF collection system so that measurements can be made relatively quickly while obtaining a useful signal to noise ratio. This was done through the implementation of a field programmable gate array (FPGA)-based demodulation system[30] and efficient collection optics described below.

A schematic of the LIF system is shown in Fig. 1. A TOPTICA TA 100 amplified tunable diode laser was modulated using a Conoptics 390–2P electro-optic modulator. The laser excited metastable Ar II ions from state $3s^2 3p^4 ({}^3P) 3d\, {}^4F_{7/2}$ (17.70 eV above the ground state) to state $3s^2 3p^4 ({}^3P) 4p^4 D^o_{5/2}$ (19.55 eV) using 668 nm light, which decayed to state $3s^2 3p^4 ({}^3P) 4s\, {}^4P_{3/2}$ (16.75 eV) resulting in 442 nm fluorescence.[32] The laser power density was approximately 30 mW/cm^2 in the observation volume. To reduce photon statistics noise to a manageable level, a relatively large collection volume was observed near the center of the chamber, approximately 1.2 cm × 1.2 cm × 1.9 cm. This was done using efficient low f-number collection optics that resulted in a photon count rate of approximately 200 MHz. To handle the high rate of photon pulses, the system was parallelized by splitting the incoming light between a pair of 16 element photomultiplier tube detectors with discriminators for each channel to reduce the chance of missed counts caused by overlapping pulses. The laser was modulated at 2 MHz giving a spectral bandwidth of 1 MHz. An FPGA-based demodulation system developed by Mattingly and Skiff[30] was used to perform the background subtraction in real-time as the data were acquired using an up/down counting technique. The FPGA is particularly useful due to its flexibility and speed. It has been configured with 32 digital inputs and a phase adjustable 2 MHz output to control the laser modulation. The signal was transferred to a computer where the time resolved arrays were time-cross-correlated and integrated into a running average. For the measurements presented, 300 000 16 ms long acquisitions were averaged for each of the 11 electrode configurations tested. Cross-correlations were convolved with a 1 ms wide Gaussian windowing function to remove uncorrelated noise from the data and then Fourier transformed to give the power spectral density (PSD).

Because the LIF signal is proportional to the density of metastable ions at the Doppler-selected velocity, the strongest fluctuation signal is observed when the laser is tuned to the part of the IVDF where the slope is the greatest. This corresponds to ions moving at the thermal speed $v_{ti} \approx 290$ m s^{-1}. LIF was used to measure the IVDF for each of the 11 configurations tested before the LIF fluctuation measurements to find the optimal laser tuning setting. In each case, ions were observed to have a generally Maxwellian velocity distribution with a temperature of 0.035 ± 0.010 eV and small flow-shifts of ≤ 100 m s^{-1}. The Doppler-selected ion velocities V_D used for the fluctuation measurements are given in Table I.

IV. RESULTS AND DISCUSSION

Measurements of fluctuation power spectra are shown in Fig. 4 for each electrode configuration. Panels on the left correspond to LIF measurements, while panels on the right show fluctuations in the current collected by the biased electrode measured with the spectrum analyzer. The frequency axes are normalized to the ion plasma frequency $f_{pi} \approx 1.0$ MHz, calculated from the average plasma density measured throughout the experiment. The vertical axes are normalized to the peak fluctuation power for each column (note the change of scale in the bottom four rows). Each spectrum analyzer trace is the average of 12 acquisitions collected between LIF measurements. The density, and thus instability frequency, drifted slightly throughout the experiment resulting in a broadening effect in the LIF and averaged spectrum analyzer measurements. Individual spectrum analyzer traces (not shown) indicate that the true fluctuation bandwidth was between 0.5 and 2.0 kHz ($5 \times 10^{-4} < \Delta f/f_{pi} < 2 \times 10^{-3}$) FWHM. Fluctuations were observed in every configuration except 11, where the electrode was electrically floating and positioned far from the viewing volume.

The observed frequency of the fluctuation peak was near $0.46 f_{pi}$ for each configuration tested. This is consistent with the theoretical prediction from the dispersion relation for each sheath polarity. For the electron sheath case, the predicted fluctuation frequency was between $0.5 f_{pi}$ and $0.6 f_{pi}$ depending on the flow speed. The small discrepancy may be caused by an error in the Langmuir probe density measurements or the approximation of the velocity distribution functions as Maxwellian in the dispersion relation. PIC simulations have shown a loss-cone type truncation in the electron velocity distribution function, which could influence the instability frequency prediction if taken into account.[23]

The ion sheath case is more complicated to interpret since the flow was not expected to be unstable at the location of the LIF

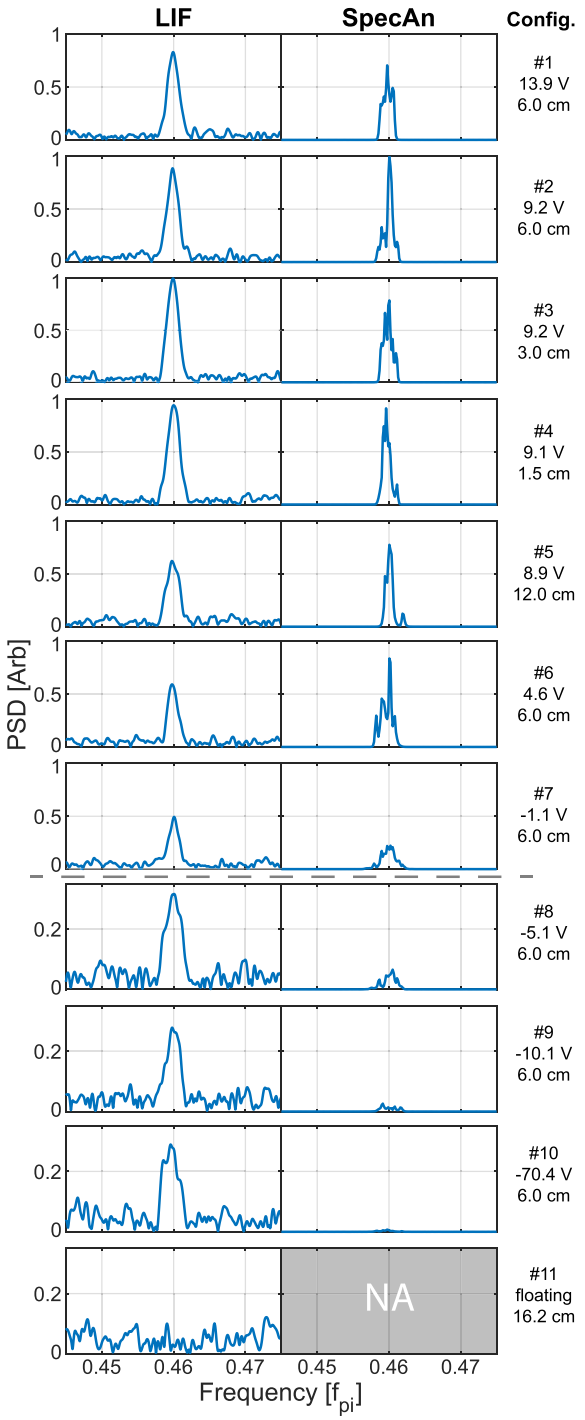

FIG. 4. LIF power spectra (left) and FFTs of the current collected by the biased electrode (right) are shown for each electrode configuration. The frequency axes are normalized to the ion plasma frequency $f_{pi} \approx 1.0$ MHz. The vertical axes are normalized to the peak fluctuation power for each column (note the change of scale in the bottom four rows). The electrode was floating in configuration 11, so there was no FFT measurement.

measurements, since the ion flow was only measured to be approximately 100 m s^{-1} ($V_i = 0.03c_s$) in this location and the electrons are not expected to have any flow in the ion presheath. However, the observed fluctuations agree with the predicted frequency in the unstable region between $0.1f_{pi}$ and $1.0f_{pi}$ depending on the flow speed. The best agreement corresponds to a flow-shift of approximately $0.7c_s$, which gives a predicted instability frequency near the observed value of $0.46f_{pi}$. A possible explanation is that the ion-acoustic waves generated in the unstable region near the electrode convect toward the boundary, reflect off the sheath, and then propagate away from the boundary. Short wavelength ion-acoustic waves are predicted to be absorbed at an ion sheath;[33–35] however, wave reflection is supported by four pieces of evidence. First, the fluctuations were excited by the electrode, since they were not observed in the control case of configuration 11 when the electrode was absent. Second, the fluctuation frequency that was observed is consistent with the predicted instability near the sheath edge, where the flow would be approximately $0.7c_s$. Third, the region near the sheath edge is the only location where the flow is unstable. Fourth, the dispersion relation predicts that the unstable modes convect toward the boundary but may reflect. These waves would propagate through the plasma but would no longer be growing once they reflect since their wave vector is against the flow direction.

Side by side comparisons between LIF and spectrum analyzer measurements show an agreement for the fluctuation frequency in each case. In addition, the amplitudes of the fluctuation peaks measured with each diagnostic follow similar trends, becoming weaker in the ion sheath cases and farther from the electrode, but are clearly not in quantitative agreement. This is expected because LIF provides measurements that are spatially resolved and only sensitive to the ions, whereas the spectrum analyzer observes the net current collected by the biased electrode, composed of a mixture of ions and electrons that depend on the bias of the electrode.

The total fluctuation power was calculated by integrating across the peak of each power spectrum shown in Fig. 4 and subtracting off the background level. The integrated fluctuation power is shown in Fig. 5, plotted against the electrode potential relative to the plasma potential in panel (a) and position in panel (b). Error bars were calculated as the standard deviation of data points divided by the square root of the number of points.

Fluctuation strength was observed to increase significantly when the electrode was biased above the plasma potential; see Fig. 5(a). This corresponds to the transition between ion and electron sheaths on the biased electrode. This is consistent with the modified electron sheath theory,[2] which predicts a significantly faster differential flow between ions and electrons in the presheath that drives stronger fluctuations than in an ion presheath. The difference between the fluctuation amplitude measured with LIF vs the spectrum analyzer in the ion sheath cases (configurations 7–10) is likely associated with the measurement technique. This is likely a result of the spectrum analyzer observing a mixture of ions and electrons, depending on the electrode bias, compared to LIF, which is only sensitive to ions. It is also noted that the two methods sample different volumes of plasma. In Fig. 5(a), the LIF viewing volume was 6 cm from the boundary, whereas the spectrum analyzer observed the current collected at the boundary. LIF fluctuations are observed to increase by a factor of approximately 4 when the electrode is biased significantly above the plasma potential compared to an

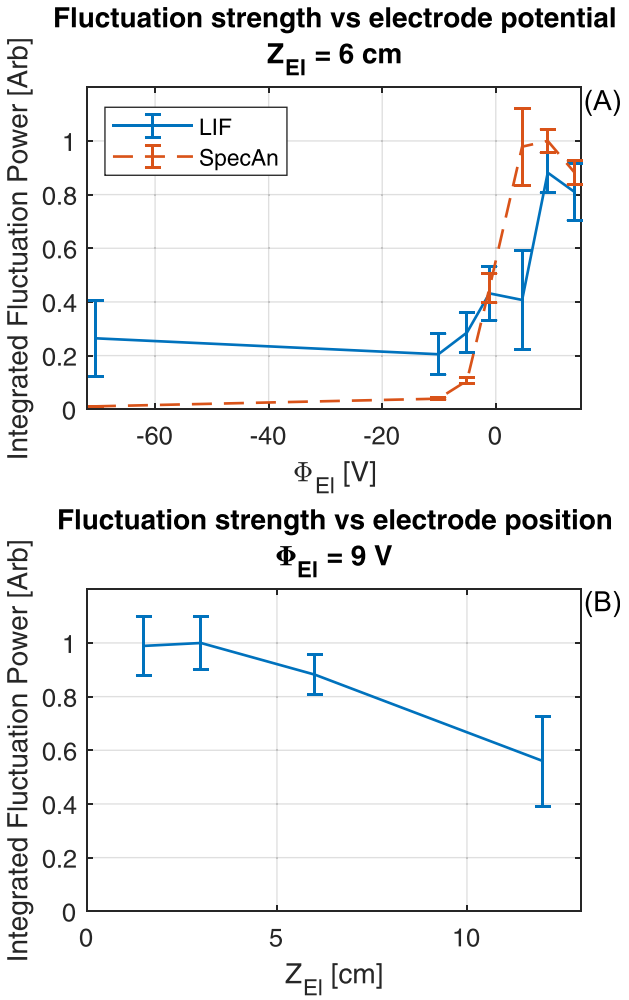

FIG. 5. Integrated fluctuation spectra are plotted showing the instability power as a function of the electrode bias (panel a) and distance from the electrode (panel b). Solid lines represent LIF measurements, and the dashed lines represent spectrum analyzer measurements. Data points for each measurement technique are normalized to the largest amplitude point from that technique.

increase by a factor of approximately 40 when measuring fluctuations in the biased electrode current.

Spatially resolved measurements of ion fluctuations in the electron presheath are shown in Fig. 5(b). The fluctuation amplitude was observed to change by less than a factor of 2 over the measurement range. This suggests a long electron presheath region, since the instability has already developed 12 cm from the electrode in this case. For reference, in the ion presheath, ions at 6 cm are observed to have a flow of approximately 100 m s^{-1} toward the electrode ($V_i = 0.03c_s$). This is consistent with the theoretical predictions of a long electron presheath in the modified theory of the electron sheath.[2]

V. CONCLUSIONS

Ion and electron rich sheaths are both predicted to have presheath regions that are susceptible to electrostatic flow-driven instabilities that generate ion-acoustic fluctuations. These instabilities have been predicted theoretically and shown in simulations; however, experimental measurements using non-perturbative diagnostics have only shown indirect evidence of these instabilities to date.[3] Our measurements of ion fluctuation spectra using LIF provide the first direct measurement of these instabilities using a non-perturbative diagnostic. We find a general agreement with the theory; fluctuations were observed in the range of frequencies predicted and have a spatial dependence that is consistent with the modified theory for the electron sheath.[2] An unexpected result was the observation of significant fluctuation power at a location in the ion presheath that was far enough from the electrode that no instability was predicted. Evidence suggests that this may be caused by waves excited near the sheath edge, where the flow is predicted to be unstable, reflecting from the sheath edge and propagating into the bulk plasma. This is a potentially significant result since it would mean that any biased probe could, in effect, act as an antenna for ion-acoustic fluctuations. This would influence many experiments and applications that are sensitive to the form of the velocity distribution function such as in the modeling of steady-state plasma conditions, plasma–surface interactions, and the interpretation of many probe-based measurements, since fluctuations are predicted to result in instability-enhanced collisions that thermalize the velocity distribution. Our measurements underscore the importance of using non-perturbative diagnostics such as LIF, since a probe may introduce ion-acoustic waves that interfere with the measurement.

Future investigations may seek to analyze the effect of a loss-cone in the electron velocity distribution function on the instability prediction in the electron presheath, as suggested by PIC simulations.[23] Future experiments may attempt to measure the group velocity of instability generated ion-acoustic waves to determine if wave reflection plays a significant role in the ion presheath.

ACKNOWLEDGMENTS

This research was supported by the Office of Fusion Energy Sciences at the U.S. Department of Energy under Contract No. DE-SC0016473.

DATA AVAILABILITY

The data that support the findings of this study are available from the corresponding author upon reasonable request.

REFERENCES

[1]S. D. Baalrud, Plasma Sources Sci. Technol. **25**, 025008 (2016).
[2]B. Scheiner, S. D. Baalrud, B. T. Yee, M. M. Hopkins, and E. V. Barnat, Phys. Plasmas **22**, 123520 (2015).
[3]C.-S. Yip, N. Hershkowitz, and G. Severn, Plasma Sources Sci. Technol. **24**, 015018 (2014).
[4]J. Glanz and N. Hershkowitz, Plasma Phys. **23**, 325 (1981).
[5]B. T. Yee, B. Scheiner, S. D. Baalrud, E. V. Barnat, and M. M. Hopkins, Plasma Sources Sci. Technol. **26**, 025009 (2017).
[6]M. A. Lieberman and A. J. Lichtenberg, *Principles of Plasma Discharges and Materials Processing*, 2nd ed. (Wiley, Hoboken, NJ, 2005), Chap. 6, pp. 165–172.
[7]K.-U. Riemann, Phys. Plasmas **4**, 4158 (1997).
[8]L. Oksuz and N. Hershkowitz, Phys. Rev. Lett. **89**, 145001 (2002).
[9]S. D. Baalrud and C. C. Hegna, Plasma Sources Sci. Technol. **20**, 025013 (2011).

[10]S. D. Baalrud, J. D. Callen, and C. C. Hegna, Phys. Rev. Lett. **102**, 245005 (2009).
[11]N. Claire, G. Bachet, U. Stroth, and F. Doveil, Phys. Plasmas **13**, 062103 (2006).
[12]S. D. Baalrud, N. Hershkowitz, and B. Longmier, Phys. Plasmas **14**, 042109 (2007).
[13]S. J. Zweben, R. J. Maqueda, A. L. Roquemore, C. E. Bush, R. Kaita, R. J. Marsala, Y. Raitses, R. H. Cohen, and D. D. Ryutov, Plasma Phys. Controlled Fusion **51**, 105012 (2009).
[14]C. Theiler, I. Furno, J. Loizu, and A. Fasoli, Phys. Rev. Lett. **108**, 065005 (2012).
[15]C.-S. Yip, J. P. Sheehan, N. Hershkowitz, and G. Severn, Plasma Sources Sci. Technol. **22**, 065002 (2013).
[16]V. I. Demidov, S. V. Ratynskaia, and K. Rypdal, Rev. Sci. Instrum. **73**, 3409 (2002).
[17]G. F. Matthews, Plasma Phys. Controlled Fusion **36**, 1595 (1994).
[18]S. Sharma, D. Gahan, P. Scullin, J. Doyle, J. Lennon, R. K. Vijayaraghavan, S. Daniels, and M. B. Hopkins, Rev. Sci. Instrum. **87**, 043511 (2016).
[19]H. M. Mott-Smith and I. Langmuir, Phys. Rev. **28**, 727 (1926).
[20]N. Hershkowitz, Phys. Plasmas **12**, 055502 (2005).
[21]K. U. Riemann, J. Phys. D **24**, 493 (1991).
[22]F. F. Chen, Plasma Sources Sci. Technol. **15**, 773 (2006).
[23]B. Scheiner, S. D. Baalrud, M. M. Hopkins, B. T. Yee, and E. V. Barnat, Phys. Plasmas **23**, 083510 (2016).
[24]R. Hood, B. Scheiner, S. D. Baalrud, M. M. Hopkins, E. V. Barnat, B. T. Yee, R. L. Merlino, and F. Skiff, Phys. Plasmas **23**, 113503 (2016).
[25]J. P. Sheehan, Y. Raitses, N. Hershkowitz, I. Kaganovich, and N. J. Fisch, Phys. Plasmas **18**, 073501 (2011).
[26]D. N. Hill, S. Fornaca, and M. G. Wickham, Rev. Sci. Instrum. **54**, 309 (1983).
[27]A. Diallo and F. Skiff, Phys. Plasmas **12**, 110701 (2005).
[28]I. U. Uzun-Kaymak and F. Skiff, Phys. Plasmas **13**, 112108 (2006).
[29]S. Mattingly and F. Skiff, Phys. Plasmas **24**, 090703 (2017).
[30]S. W. Mattingly and F. Skiff, Rev. Sci. Instrum. **89**, 043508 (2018).
[31]F. Chu and F. Skiff, Phys. Plasmas **25**, 013506 (2018).
[32]A. Kramida, Y. Ralchenko, and J. Reader, and NIST ASD Team, *NIST Atomic Spectra Database (Ver. 5.6.1)* (National Institute of Standards and Technology, Gaithersburg, MD, 2018).
[33]B. Bertotti, M. Brambilla, and A. Sestero, Phys. Fluids **9**, 1428 (1966).
[34]O. Ishihara, I. Alexeff, H. J. Doucet, and W. D. Jones, Phys. Fluids **21**, 2211 (1978).
[35]J. Berumen and F. Skiff, Phys. Plasmas **25**, 122102 (2018).